Novel translational phenotypes and biomarkers for creatine transporter deficiency

Raffaele Mazziotti[1,2]‡, Francesco Cacciante[3]‡, Giulia Sagona[1,4]‡, Leonardo Lupori[3], Mariangela Gennaro[2], Elena Putignano[2], Maria Grazia Alessandrì[4], Annarita Ferrari[4], Roberta Battini[4,5], Giovanni Cioni[4,5], Tommaso Pizzorusso[1,2], Laura Baroncelli[2,4*]

[1] Department of Neuroscience, Psychology, Drug Research and Child Health NEUROFARBA, University of Florence, I-50135, Florence, Italy

[2] Institute of Neuroscience, National Research Council (CNR), I-56124, Pisa, Italy

[3] BIO@SNS lab, Scuola Normale Superiore di Pisa, I-56125 Pisa, Italy

[4] Department of Developmental Neuroscience, IRCCS Stella Maris Foundation, I-56128, Pisa, Italy

[5] Department of Clinical and Experimental Medicine, University of Pisa, Pisa, Italy

*To whom correspondence should be addressed: baroncelli@in.cnr.it.

‡These authors equally contributed to the work

Corresponding author:

Laura Baroncelli

Institute of Neuroscience, National Research Council (CNR)

via Moruzzi 1, Pisa I-56124, Italy.

Email: baroncelli@in.cnr.it

Tel: +390 503 153199 Fax: +390 503 153220

Running title: Biomarkers for metabolic disorders

© The Author(s) (2020). Published by Oxford University Press on behalf of the Guarantors of Brain.
This is an Open Access article distributed under the terms of the Creative Commons Attribution Non-Commercial License (http://creativecommons.org/licenses/by-nc/4.0/), which permits non-commercial re-use, distribution, and reproduction in any medium, provided the original work is properly cited. For commercial re-use, please contact journals.permissions@oup.com

Downloaded from https://academic.oup.com/braincomms/advance-article/doi/10.1093/braincomms/fcaa089/5866973 by guest on 16 August 2020

Abstract

Creatine transporter deficiency is a metabolic disorder characterized by intellectual disability, autistic-like behavior and epilepsy. There is currently no cure for creatine transporter deficiency, and reliable biomarkers of translational value for monitoring disease progression and response to therapeutics are sorely lacking. Here, we found that mice lacking functional creatine transporter display a significant alteration of neural oscillations in the EEG and a severe epileptic phenotype that are recapitulated in patients with creatine transporter deficiency. In-depth examination of knock-out mice for creatine transporter also revealed that a decrease in EEG theta power is predictive of the manifestation of spontaneous seizures, a frequency that is similarly affected in patients compared to healthy controls. Additionally, knock-out mice have a highly specific increase of hemodynamic responses in the cerebral cortex following sensory stimuli. Principal Component and Random Forest analysis highlighted that these functional variables exhibit a high performance in discriminating between pathological and healthy phenotype. Overall, our findings identify novel, translational and non-invasive biomarkers for the analysis of brain function in creatine transporter deficiency, providing a very reliable protocol to longitudinally monitor the efficacy of potential therapeutic strategies in preclinical, and possibly clinical, studies.

Keywords:

Creatine transporter deficiency, biomarkers, epilepsy, EEG, optical imaging

List of abbreviations: ASD: autism spectrum disorder; BOLD: blood oxygenation level dependent; CI: confidence interval; Cr: creatine; Crn: creatinine; CrT: creatine transporter; CTD: creatine transporter deficiency; C3: central 3; EDF: European Data Format; FFT: Fast Fourier Transform; fMRI: functional magnetic resonance imaging; fNIRS: functional near-infrared spectroscopy; FP1: frontopolar 1; IOS: intrinsic optical imaging; ip: intraperitoneal; KA: kainic acid; KO: knock-out; LED: light emitting diode; MRS: magnetic resonance spectroscopy; O1: occipital 1; PCA: principal component analysis; PND: postnatal day; RF: Random Forest; RM: repeated measures; ROI: region of interest; SD: standard deviation; T3: temporal 3; VEP: visually evoked potential; WT: wild-type.

Downloaded from https://academic.oup.com/braincomms/advance-article/doi/10.1093/braincomms/fcaa089/5866973 by guest on 16 August 2020

Introduction

A disruption of brain energy metabolism has been associated with multiple psychiatric and neurological disorders, including for instance schizophrenia, Rett syndrome and a subset of autism spectrum disorders (ASDs; e.g., Müller and Can, 2014; Rose et al., 2018; Dwir et al., 2019). Creatine (Cr) Transporter Deficiency (CTD) is a recessive X-linked inherited alteration of metabolism (OMIM #300352), characterized by greatly diminished or undetectable levels of Cr in the brain, and presenting with early intellectual disability, symptoms overlapping with ASDs, seizures and motor abnormalities (Cecil et al., 2001; van de Kamp et al., 2014). CTD is caused by mutations in *Slc6a8* gene and loss of function of Cr transporter 1 (CrT), which transports Cr both across the blood-brain barrier and into the cells (Nash et al., 1994). The prevalence of CTD is unknown, but the disorder has been estimated to account for 1-2% of males with non-syndromic mental disability (van de Kamp et al., 2014). Although rare, CTD represents a major issue in health-care, as it is a chronic illness requiring life-long care and resulting in a large impact on the quality of life of both patients and caregivers, as well as a burden on the health-care system. There are no therapies for this disorder and the current standard of care is a palliative approach for managing seizures and behavioural problems (van de Kamp et al., 2014). Previous attempts to rescue Cr content in the brain of CTD patients by exploiting nutritional supplements or Cr analogs have met with very limited success (Chilosi et al., 2008; Mercimek-Mahmutoglu et al., 2010; Kurosawa et al., 2012; Valayannopoulos et al., 2012; Dunbar et al., 2014; Jaggumantri et al., 2015). Recently, CrT knock-out murine models that recapitulate many aspects of the human disease have become available, supporting the preclinical development of therapeutics and a better understanding of CTD pathophysiology (Skelton et al., 2011; Kurosawa et al., 2012; Baroncelli et al., 2016: Udobi et al., 2018; Molinaro et al., 2019). However, the efficacy study of novel potential treatments is hindered by the scarcity of unbiased, quantitative biomarkers for monitoring brain development and function.

EEG and sensory-evoked responses are readily applicable to humans and widely used for non-invasive assessment of cortical function, making electrophysiological measurements or functional imaging ecologically ideal translational tools for functional analyses in children with neurodevelopmental disorders (Nelson and McCleery, 2008; Lloyd-Fox et al., 2010; Vanderwert and Nelson, 2014). Accordingly, previous studies reported that a standardized inspection of EEG and cortical responses to sensory stimuli is suitable to reveal, both in animal models and patients, stage-specific alterations in other disorders affecting neurodevelopment (Bosl et al., 2011; Durand et al., 2012; LeBlanc et al., 2015; Boggio et al., 2016; Mazziotti et al., 2017; Bowman and Varcin, 2018; Lupori et al., 2019). Abnormal EEG waveforms have been previously documented in CTD patients, indicating diffuse slowing, interictal theta activity, aspecific sharp abnormalities, and

Downloaded from https://academic.oup.com/braincomms/advance-article/doi/10.1093/braincomms/fcaa089/5866973 by guest on 16 August 2020

focal/generalized paroxysmal or slow abnormalities (Schiaffino et al., 2005; Póo et al., 2006; Mancardi et al., 2007; Fons et al., 2009; Leuzzi et al., 2013). However, a quantitative examination of CTD electroclinical features is still missing.

Here, we performed an extensive functional analysis in knock-out mice lacking CrT ($CrT^{-/y}$) and CTD patients identifying reliable biomarkers that could potentially be used to evaluate therapeutics pre-clinically as well as clinically.

Downloaded from https://academic.oup.com/braincomms/advance-article/doi/10.1093/braincomms/fcaa089/5866973 by guest on 16 August 2020

Materials and methods

Animals

We used male mice hemizygous for CrT exons 5-7 deletion ($CrT^{-/y}$ or knock-out (KO)) on a C57Bl6J background (Baroncelli et al., 2014), and their wild-type (WT; $CrT^{+/y}$) littermates. Animals in each experimental group came from different litters, with a minimum of three litters to prevent possible litter effects. Animals were maintained at 22°C under a 12-h light–dark cycle (average illumination levels of 1.2 cd/m^2) and housed in standard cages according to current regulations about animal welfare. Food (4RF25 GLP Certificate, Mucedola) and water were available *ad libitum*. Genomic DNA was isolated from mouse tail (Dneasy Blood and Tissue Kit, Qiagen, USA) and genotyping was performed as previously described (Baroncelli et al., 2014). All experiments were carried out in accordance with the European Directive of 22 September 2010 (EU/63/2010) and were approved by the Italian Ministry of Health (authorization number 507/2018-PR).

EEG recordings in mice

A two-channel headmount (8201, Pinnacle Technology) for EEG recordings was placed on the skull of mice anesthetized with isoflurane (1-3%). EEG electrodes were stainless steel screws implanted epidurally over the frontal and the occipital areas. EEG signals were recorded using a preamplifier (8202-SL) connected to a data acquisition system (8206, Pinnacle Technology) and Sirenia Software 1.7.9 (Pinnacle Technology). Signals were recorded at 400 Hz sampling frequency to evaluate baseline (spontaneous) activity for 24 hours followed by treatment with i.p. kainic acid (KA) at 10 mg/kg to evoke seizure activity. Video was recorded in parallel during the entire duration of the EEG assessments. For the analysis of baseline EEG, signals were segmented in 30 second epochs. The vigilance state in each epoch was manually classified as active wake, passive wake or sleep, based on the inspection of video recordings by an operator blind to the genotypes. EEG signals were converted into power spectra by Fast Fourier Transform (FFT) for at least 12 epochs in each light/dark cycle and wake/sleep condition. Consecutive epochs of the same vigilance

state were selected to be spaced at least 10 minutes apart between each other. The spectra were normalized to the total power of the signal. The power spectra were averaged over subjects in each light/dark cycle and wake/sleep condition at frequency ranges divided into five bands as follows: 0.5–4 (delta), 4–8 (theta), 8–12 (alpha), 12–30 (beta), and 30–45 (gamma) Hz (Kadam et al., 2017). A correlation matrix of EEG spectral power in $CrT^{-/y}$ and WT animals was obtained using Spearman correlation, with Benjamini-Hochberg adjustment (Python, *scipy* library). To quantify both baseline (spontaneous) and KA-evoked seizure episodes we used Sirenia Seizure Pro 1.8.4 (Pinnacle Technology). The baseline period of each animal was used as a cutoff threshold (mean line length + 8xSD). Events in the 2-10 Hz frequency range, with a line length higher than the defined threshold, and lasting at least 10 seconds were identified as seizures. At the behavioral level, seizures were scored according to Racine scale (Racine, 1972). Seizures of stage 1 and 2 were classified as tonic events, seizures of stage 3 were assigned to clonic events and seizures of stage 4, 5 and 6 were categorized as tonic-clonic events.

Patients

Five subjects with CTD aged to the present date between 7.7 and 22.7 years were diagnosed at IRCCS Stella Maris Foundation at the age ranging between 5.1 and 9 years (mean age = 7.2 years; SD = 1.8 years). All patients showing clinical, neurochemical (Cr/Crn urine levels and lack of brain Cr at ^{1H}MRS) and genetical diagnosis of CTD have been recruited in this study and matched with twelve healthy subjects. The mean age of controls was 7.7 years (SD = 2.3 years). A breakdown of demographics for CTD patients is reported in Table 1. Data have been anonymized using an alphanumeric code. Despite the occurrence of seizures with predominant focal onset in patients 1, 2 and 5, no specific EEG pattern can be recognized in the clinical observation of interictal video-EEG. The experiment has been subjected to approval by the Ethics Board (201/2019, Pediatric Ethics Board of Tuscany) and has been performed in accordance with the Declaration of Helsinki.

EEG recordings in patients

EEG recordings were performed as part of routine examination of patients with intellectual disability and language deficits. Data were collected using a Micromed or Grass EEG recording system. Gold ring electrodes were placed following the international 10–20 convention for a 32-channel cap and signals were recorded at a sampling rate of 500 Hz. For this analysis, we used the first EEG recorded at the time of diagnosis; thus, patients were not prescribed yet anticonvulsant medications. The spectral power values in the same frequency bands described above for mice were evaluated in humans (Kadam et al., 2017). EEG recordings were screened and divided into artefact-

Downloaded from https://academic.oup.com/braincomms/advance-article/doi/10.1093/braincomms/fcaa089/5866973 by guest on 16 August 2020

free segments (10s duration for eyes closed condition, 20s duration for eyes open and sleep conditions). EEG signal was then exported in European Data Format (EDF) and subjected to FFT. Power spectra were estimated by averaging at least 8 segments for each behavioral state. The spectra were normalized to the total power of the signal. Data analysis was performed by an operator blind to the genotype.

Intrinsic optical signal (IOS) imaging and visually evoked potentials (VEPs)

Surgery was performed as previously described (Mazziotti et al., 2017). Isoflurane was used as anaesthesia. A thin layer of cyanoacrylate was poured over the exposed skull to affix a custom-made metal ring (9 mm internal diameter) in correspondence with the binocular visual cortex and a drop of transparent nail polish was used to improve the optical access. IOS recordings were performed under isoflurane (0.5-1%) and chlorprothixene anesthesia (1.5 mg/kg, i.p.) longitudinally in each animal at postnatal day (PND) 40, PND110 and PND180. Images were visualized using a custom Leica microscope (Leica Microsystems). The animals were secured under the objective using a ring-shaped magnet mounted on an arduino-based imaging chamber. Red light illumination (630 nm) was obtained with 8 individually addressable LEDs (WS2812) fixed to the objective (Leica Z6 APO coupled with a Leica PanApo 2.0X 10447170) by a custom 3D printed conical holder (Lupori et al., 2019). Visual stimuli were generated using Matlab Psychtoolbox and presented on a monitor placed 13 cm away from the eyes of the mouse. Sinusoidal wave gratings were presented in the binocular portion of the visual field with spatial frequency 0.03 cyc/deg, mean luminance 20 cd/m^2 and contrast up to 90%. The stimulus consisted in the abrupt contrast reversal of a grating with a temporal frequency of 4 Hz for 1 s. Frames were acquired at 30 fps with a resolution of 512×512 pixels. The signal was averaged for at least 80 trials. Fluctuations of reflectance (R) for each pixel were computed as the normalized difference from the average baseline ($\Delta R/R$). A region of interest (ROI) was calculated on the mean image of contralateral eye response by selecting the pixels in the lowest 30% $\Delta R/R$ of the range between the maximal and minimal intensity pixel, and mean evoked response was quantitatively estimated as the average intensity within the ROI. See (Mazziotti et al., 2017) for further details on signal analysis. A separate group of animals were used for VEP experiments at PND110 using Cheetah 32 (Neuralynx) recording system (Mazziotti et al., 2017).

Behavioural tests

All behavioural tests were performed as previously reported (Baroncelli et al., 2016).

Downloaded from https://academic.oup.com/braincomms/advance-article/doi/10.1093/braincomms/fcaa089/5866973 by guest on 16 August 2020

Y-maze- We used a Y-shaped maze with three symmetrical plastic arms at a 120-degree angle (26 x 10 x 15 cm). Mice were allowed to freely explore the maze for 8 min. Video recordings (Noldus Ethovision XT) were used for offline blind analysis. An arm entry was defined as all four limbs within the arm. A triad was defined as a set of three arm entries, when each entry was to a different arm of the maze. The number of arm entries and the number of triads were recorded in order to calculate the alternation percentage. *Morris water maze*- Mice were trained for four trials per day and for a total of 7 days in a circular water tank (diameter, 120 cm; height, 40 cm), filled to a depth of 25 cm with water (21-22°C) added with atoxic white paint. Four alternative starting positions defined the division of the tank into four quadrants. A square clear Perspex platform (11x11 cm) was submerged 0.5 cm below the water surface and placed at the midpoint of the target quadrant. Mice were allowed up to 60 s to locate the escape platform, and their swimming paths were recorded by the Noldus Ethovision system. On the last trial (probe trial), the platform was removed and the swimming paths were recorded over 60 s. *Rotarod*- Mice were placed on a drum with increasing rotation speed from 4 to 40 rpm in 10 min. The time spent on the drum was recorded by an automated unit. Four consecutive trials with an inter-trial interval of 5 min were performed in the same day.

Experimental design

The same animals were subjected to longitudinal IOS recordings at PND40, PND110 and PND180. At least four days after the completion of each IOS recording, the animals were each subjected to serial neurobehavioural assessments of cognitive and psychomotor functions (Y maze, Rotarod, Morris Water Maze (PND110 and PND180 only)). At the end of the experimental schedule (PND200), EEG recordings were performed. Data analysis was performed *a posteriori* by an operator blind to the genotype of mice.

Machine learning-based classification

Scikit-learn, a Python-based library (http://scikit-learn.org/stable/), was used to compute both principal component analysis (PCA) and train the classification model. The model is a supervised machine learning algorithm called Random Forest (RF) that is based on multiple decision tree learning. We used the Scikit-learn implementation for this algorithm, called *ExtraTreesClassifier* function. To determine an optimal set of hyparameters for the classifier we used the function *RandomizedSearchCV* on the dataset with all the variables. Then, we applied the RF classifier adopting the function *cross_val_score* with cv = 3 to perform 3-fold cross-validation. To calculate feature importance in classifier decision, we used the attribute *feature_importance* that is an

Downloaded from https://academic.oup.com/braincomms/advance-article/doi/10.1093/braincomms/fcaa089/5866973 by guest on 16 August 2020

instance of the *ExtraTreesClassifier* expressing the fraction of relative importance for each feature. Data from all ages of phenotyping (PND40, PND110 and PND180) were averaged together.

Statistical analysis

For the assessments in mice, we estimated the sample size needed for each experiment by performing a power analysis using G*Power (α=0.05, β=0.2). The estimate of the expected difference between the experimental groups was based on the knowledge of values of the studied parameter obtained historically in the same laboratory in $CrT^{-/y}$ animals. For each parameter, we estimated the minimal difference that would be biologically relevant considering the impact of the possible difference on the animals' brain function and behavior. Considering the rarity of CTD and the few patients studied herein, we did not perform a specific statistical analysis for the patient assessments. All statistical analyses of the results were performed using GraphPad Prism 8.0.1 and Python. Differences between two groups were assessed with a two-tailed t-test. Multiple t-test with Benjamini, Krieger and Yekutieli adjustment were used for the analysis of EEG spectral power in mice. Multiple t-test were used for the analysis of EEG spectral power in patients. Correlation analysis was obtained using Spearman correlation, with Benjamini-Hochberg adjustment. The significance of factorial effects and differences among more than two groups were evaluated with ANOVA/RM ANOVA followed by post hoc Holm-Sidak test. Fisher's exact test and χ^2 test were used to compare sampling distributions. Rank transformation was exploited for data not normally distributed. The level of significance was $p < 0.05$.

Data availability

The datasets generated during the current study are available from the corresponding author on reasonable request.

Results

CrT deficiency causes an alteration of cortical oscillations in mice and humans

We performed 24h video-EEG recordings in awake, freely-moving adult mice with a view to thoroughly examining basal brain activity of WT and $CrT^{-/y}$ animals (Fig. 1a). We found that $CrT^{-/y}$ animals show significantly altered power in a wide range of EEG frequencies, including theta (4-8 Hz), alpha (8-12 Hz), beta (12-30 Hz) and gamma (30-45 Hz) bands, both during active/passive wake and sleep, regardless of the light or dark phase (Fig. 1b; Supplementary Fig.1,2). Interestingly, a correlation matrix to summarize spectral density data in WT and $CrT^{-/y}$ mice suggests an anomalous synchronization of brain activity and, possibly, functional connectivity in

Downloaded from https://academic.oup.com/braincomms/advance-article/doi/10.1093/braincomms/fcaa089/5866973 by guest on 16 August 2020

the brain of CrT$^{-/y}$ animals. Spectral densities in CrT$^{-/y}$ mice showed a lower proportion of positive correlations (blue patches; 59.8% vs. 75.8%) and a higher percentage of inversely correlated frequency bands (red patches; 59.8% vs. 40.2%) compared to WT animals (Supplementary Fig. 3).

To obtain a clinical validation of results obtained in the mouse model, we evaluated EEG data from CTD children diagnosed at the IRCCS Stella Maris Foundation (Fig. 1c). We report a significant difference between CTD patients and age-matched controls for frequency oscillations in the delta, theta, alfa and gamma bands. These alterations are particularly prominent in the signal recorded from the central (C3) electrode, but some of them are recurring at the temporal (T3) and occipital (O1) recording sites as well (Fig. 1d; Supplementary Fig. 4-6).

CrT$^{-/y}$ mice display a spontaneous epileptic phenotype

We found that approximately 30% of CrT$^{-/y}$ animals showed at least one spontaneous seizure detectable both at behavioral level and as epileptiform activity in EEG during baseline recording (24h), whereas no ictal events were detected in WT littermates (Fig. 2a). Notably, CrT$^{-/y}$ mice with the spontaneous epileptic phenotype display on average one electrographical seizure every 2h (Fig. 2b), with a mean duration of about 20 s (Fig. 2c), that simultaneously presented as clonic or tonic-clonic convulsions at the behavioural level in most cases (1.4% of tonic seizures, 54.3% of clonic seizures, 44.3% of tonic-clonic seizures; Video 1,2). The larger portion of spontaneous seizures occurred during passive wake (7.1% during active wake, 62.9% during passive wake, 30.0% during sleep). The stratification of power spectra revealed a specific decrease of theta band in CrT$^{-/y}$ animals displaying spontaneous epilepsy (Fig. 2d-i). Moreover, CrT$^{-/y}$ mice presented a distinct response to kainic acid (KA) challenge compared to WT mice. Statistical analysis revealed a significant effect of genotype with a higher Racine behavioural score following KA administration (Fig. 3a), lower latency to epileptiform activity bursts (Fig. 3b), and higher frequency and mean duration of epileptiform bursts in CrT$^{-/y}$ with respect to WT mice (Fig. 3c,d). In addition, the distribution of seizure severity was significantly different between the two groups with CrT$^{-/y}$ mice presenting a high percentage of tonic-clonic seizures (Fig. 3e).

Taken together, these data reveal that CrT$^{-/y}$ mice exhibit spontaneous seizures and increased susceptibility to pro-convulsant treatment. Moreover, the power of theta EEG band in CrT$^{-/y}$ animals appears to be predictive of spontaneous seizures phenotype.

Altered neurovascular coupling is present in CrT$^{-/y}$ mutants

We examined cortical responses to visual stimulation using intact skull IOS imaging in juvenile (PND40) CrT$^{-/y}$ animals. Fig. 4a shows typical examples of responses from CrT$^{-/y}$ and age-matched

Downloaded from https://academic.oup.com/braincomms/advance-article/doi/10.1093/braincomms/fcaa089/5866973 by guest on 16 August 2020

WT littermates. Data analysis revealed that IOS amplitude of the responses driven by contralateral eye stimulation was significantly higher in $CrT^{-/y}$ compared to control mice and the effect was particularly evident at higher contrasts of visual stimuli (Fig. 4b). We longitudinally tracked visual responses in the same animals as they aged using the 90% contrast visual stimuli. The response to the contralateral eye showed a similar pattern at PND110 and PND180 with a significantly increased amplitude in $CrT^{-/y}$ compared to WT mice (Fig. 4c). Moreover, the latency to response peak was higher in $CrT^{-/y}$ at PND110 and PND180 (Fig. 4d). These results show that hemodynamic response is markedly altered in the cortex of mutant animals, and that this phenotype progresses with age. To clarify whether this is related to a corresponding change of ongoing neuronal activity, we assessed visual responses in a separate group of adult (PND110) $CrT^{-/y}$ mice using intracortical visually-evoked potential (VEP) recordings. Data quantification revealed comparable VEP amplitude and latency in $CrT^{-/y}$ and WT animals (Fig. 4e,f).

A Random Forest classifier quantify robustness of CTD biomarkers

Longitudinal IOS imaging was conducted along with serial neurobehavioural assessments of cognitive and psychomotor functions (Y maze, Rotarod, Morris Water Maze). At the end of the experimental schedule, EEG recordings were performed in the same animals at PND180. Results of behavioural testing confirmed what was previously reported by our group (Baroncelli et al., 2016; Supplementary Fig. 7-9). To evaluate the reliability of the behavioural phenotype, imaging and electrophysiological recordings as biomarkers of CTD disorder, we computed accuracy using a Random Forest (RF) binary classifier, a supervised machine-learning algorithm for data classification. When trained with the entire dataset, the algorithm showed a remarkable capability to discriminate between $CrT^{-/y}$ and WT animals (Full; accuracy = 95.67%; Fig. 5b). As a control, we also repeated the procedure after bootstrapping the dataset (Bootstrap; accuracy = 54.86%). We then assessed the discriminative performance of smaller subsets of data dividing the entire dataset in behavioural (Behaviour), imaging (IOS) and electrophysiological (EEG) variables. We found that behavioural (accuracy = 95.45%), IOS (accuracy = 90.84%) and EEG (accuracy = 88.1%) models showed significantly better performance than the bootstrap condition, establishing the robustness and reliability of these phenotypes in our mouse model (Fig. 5a,b). Importantly, the analysis of feature importance highlighted that the most informative variables are Y maze, IOS amplitude and alpha band (night, active wake) in EEG recordings (Fig. 5c).

Downloaded from https://academic.oup.com/braincomms/advance-article/doi/10.1093/braincomms/fcaa089/5866973 by guest on 16 August 2020

Discussion

Quantitative biomarkers measuring cortical function are a fundamental tool for the development of therapeutics, and different techniques have been recently and successfully introduced in clinical and research settings for neurodevelopmental disorders (Bosl et al., 2011; Durand et al., 2012; Jeste et al., 2015; LeBlanc et al., 2015; Boggio et al., 2016; Mazziotti et al., 2017; Sinclair et al., 2017; Bowman and Varcin, 2018; Lupori et al., 2019). Following this approach, we report novel functional CTD biomarkers capable of classifying animal genotypes at single subject level with high accuracy and sensitivity (> 85%), and to measure disease progression and amelioration. These tools may be of high translational value for future preclinical studies of CTD, and also more broadly for neurodevelopmental disorders presenting with cognitive dysfunction, autistic-like features and brain hyperexcitability.

The clinical relevance of the spectral changes of EEG signal apparent in $CrT^{-/y}$ mice was demonstrated by our findings showing a comparable dysfunction of neural oscillations in CTD patients. More specifically, theta and alpha power was decreased in the cerebral cortex of $CrT^{-/y}$ mice compared to WT animals, whereas beta and gamma power was increased, highlighting a transition from physiological to pathological network activity similar to that observed in other neurodevelopmental disorders and patients in the autistic spectrum (Jeste et al., 2015; Sinclair et al., 2017). Importantly, theta and alpha bands were altered in the same direction in mice and patients, identifying a possible "network biomarker" of CTD disorder. Moreover, we demonstrated that $CrT^{-/y}$ mice display an epileptic phenotype, with spontaneous seizure occurrence and increased susceptibility to kainic acid, as assessed through behavioral observation and video-EEG recordings in awake animals. Since epilepsy is common in CTD (van de Kamp et al., 2014) and seizures are one of the symptoms with the greatest impact on quality of life of patients and caregivers, these findings fill a gap in the current literature and expand the translational validity of our CTD murine model. The stratification of animals based on the manifestation of spontaneous seizures revealed that epileptic mice exhibit a specific decrease of theta power band with respect to non-epileptic animals. This result is in agreement with previous literature showing that changes in theta band power can be predictive of epilepsy (Bettus et al., 2008; Milikovsky et al., 2017).

Since the timing of rhythmic activity in cortical networks strongly affects the coordination of neuronal responses throughout the cortex, the EEG alterations found in CTD mice and patients establish a robust link between alterations in brain oscillatory activity and the pervasive cognitive and behavioral impairment of this condition, suggesting that a derangement in local and long-range cortical connectivity and plasticity could be a good candidate to explain at the network level the pathological endophenotype of CTD (e.g., Jensend and Tesche, 2002; Klimesch et al., 2007;

Downloaded from https://academic.oup.com/braincomms/advance-article/doi/10.1093/braincomms/fcaa089/5866973 by guest on 16 August 2020

Summerfield and Egner, 2009; Uhlhaas et al., 2009; Jensen and Mazaheri, 2010; Güntekin et al., 2013; Nicolás et al., 2019). The increase of beta and gamma power could seem at odds with the observed cognitive deficits and natural history of CTD, but excessive beta/gamma activity was previously associated with increased brain excitability and seizures (Willoughby et al., 2003; Maheshwari et al., 2016). In summary, the observed EEG abnormalities may be related to different symptoms in CTD. Future studies analyzing the effects of specific pharmacological approaches (such as anti-convulsant drugs) on EEG components in CTD patients are needed to further test this notion.

We also found a highly specific increase of cortical IOS responses in $CrT^{-/y}$ mice. Since IOS imaging measures BOLD signals, these data suggest that the assessment of brain metabolic consumption might represent a further non-invasive and sensitive biomarker for the analysis of brain function in CTD. In light of the ubiquitous expression of *Slc6a8* gene in the brain at the cellular and regional level (Mak et al., 2009), the normal VEP amplitude recorded in the visual cortex of $CrT^{-/y}$ mice suggests that glial and vascular cells might be the cellular basis of altered IOS. Accordingly, the forced metabolic phenotype and the resultant increase of cellular oxidative stress observed in the brain of $CrT^{-/y}$ animals (Giusti et al., 2019) could dynamically upregulate the cerebral blood flow stimulating vasodilation (Watts et al., 2018). Abnormal neurovascular coupling could significantly affect fMRI responses in CTD patients and represent another CTD biomarker of relatively easy assessment in children using functional near infrared spectroscopy (fNIRS; Lloyd-Fox et al., 2010; Vanderwert and Nelson, 2014).

Using a Random Forest machine-learning algorithm for data classification, we showed that behavioural, imaging and EEG assessment can be used to automatically classify subjects. Since ease of testing is a key factor in complex multidose assessments, we also showed that smaller subsets of variables could reach a similar discriminative performance.

Overall, our findings identify novel, translational and non-invasive biomarkers for the investigation of brain function in CTD. Despite the availability of reliable tools for CTD diagnosis, including biochemical, magnetic resonance spectroscopy and genetic analyses, the biomarkers discovered in this work will have a fundamental impact in the research and clinical setting at multiple levels: (i) their evaluation will allow clinicians to optimize the follow-up of patients, recognizing possible alterations of brain circuits during the progression of CTD disorder; (ii) the study of EEG pattern could be predictive of the epileptic phenotype; (iii) the combination of behavioural, IOS and EEG testing provides a very reliable protocol to longitudinally monitor the efficacy of potential therapeutic strategies in preclinical, and possibly clinical, studies. It is worth noting that much effort has been invested so far in the research of therapeutic strategies aimed at

Downloaded from https://academic.oup.com/braincomms/advance-article/doi/10.1093/braincomms/fcaa089/5866973 by guest on 16 August 2020

replenishing brain Cr levels, but efficacy studies of pharmacological approaches targeting specific pathogenetic mechanisms of CTD disorder need to rely on direct measurements of brain function.

Acknowledgements

We are grateful to Dr. Minh-Ha T. Do, Dr. John McKew, Dr. Eleonora Vannini and Dr. Gabriele Sansevero for critical reading of the manuscript and stylistic revision. We thank Francesca Biondi and Elena Novelli for technical support.

Funding information

This research has been supported by grant GR-2017-02364378 funded by the Italian Ministry of Health, by Telethon grant GGP19177, by grant #1822 funded by Jerome Lejeune Foundation to LB, and by a grant from Lumos Pharma to TP and LB.

Competing interests

The authors report no competing interests, except for funding obtained to carry out the research.

References

Baroncelli L, Alessandrì MG, Tola J, Putignano E, Migliore M, Amendola E, et al. A novel mouse model of creatine transporter deficiency. F1000Res 2014; 3: 228.

Baroncelli L, Molinaro A, Cacciante F, Alessandrì MG, Napoli D, Putignano E, et al. A mouse model for creatine transporter deficiency reveals early onset cognitive impairment and neuropathology associated with brain aging. Hum Mol Genet 2016; 25: 4186–4200.

Bettus G, Wendling F, Guye M, Valton L, Régis J, Chauvel P, et al. Enhanced EEG functional connectivity in mesial temporal lobe epilepsy. Epilepsy Res 2008; 81: 58–68.

Boggio EM, Pancrazi L, Gennaro M, Lo Rizzo C, Mari F, Meloni I, et al. Visual impairment in FOXG1-mutated individuals and mice. Neuroscience 2016; 324: 496–508.

Bosl W, Tierney A, Tager-Flusberg H, Nelson C. EEG complexity as a biomarker for autism spectrum disorder risk. BMC Med 2011; 9: 18.

Downloaded from https://academic.oup.com/braincomms/advance-article/doi/10.1093/braincomms/fcaa089/5866973 by guest on 16 August 2020

Bowman LC, Varcin KJ. The Promise of Electroencephalography for Advancing Diagnosis and Treatment in Neurodevelopmental Disorders. Biol Psychiatry Cogn Neurosci Neuroimaging 2018; 3: 7–9.

Cecil KM, Salomons GS, Ball WS Jr, Wong B, Chuck G, Verhoeven NM, et al. Irreversible brain creatine deficiency with elevated serum and urine creatine: a creatine transporter defect? Ann Neurol 2001; 49: 401–404.

Chilosi A, Leuzzi V, Battini R, Tosetti M, Ferretti G, Comparini A, et al. Treatment with L-arginine improves neuropsychological disorders in a child with creatine transporter defect. Neurocase 2008; 14: 151–161.

Dunbar M, Jaggumantri S, Sargent M, Stockler-Ipsiroglu S, van Karnebeek CDM. Treatment of X-linked creatine transporter (SLC6A8) deficiency: systematic review of the literature and three new cases. Mol Genet Metab 2014; 112: 259–274.

Durand S, Patrizi A, Quast KB, Hachigian L, Pavlyuk R, Saxena A, et al. NMDA receptor regulation prevents regression of visual cortical function in the absence of Mecp2. Neuron 2012; 76: 1078–1090.

Dwir D, Giangreco B, Xin L, Tenenbaum L, Cabungcal J-H, Steullet P, et al. MMP9/RAGE pathway overactivation mediates redox dysregulation and neuroinflammation, leading to inhibitory/excitatory imbalance: a reverse translation study in schizophrenia patients [Internet]. Mol Psychiatry 2019Available from: http://dx.doi.org/10.1038/s41380-019-0393-5

Fons C, Sempere A, Sanmartì FX, Arias A, Póo P, Pineda M, et al. Epilepsy spectrum in cerebral creatine transporter deficiency. Epilepsia 2009; 50: 2168-2170.

Giusti L, Molinaro A, Alessandrì MG, Boldrini C, Ciregia F, Lacerenza S, et al. Brain mitochondrial proteome alteration driven by creatine deficiency suggests novel therapeutic venues for creatine deficiency syndromes. Neuroscience 2019; 409: 276–289.

Downloaded from https://academic.oup.com/braincomms/advance-article/doi/10.1093/braincomms/fcaa089/5866973 by guest on 16 August 2020

Güntekin B, Emek-Savaş DD, Kurt P, Yener GG, Başar E. Beta oscillatory responses in healthy subjects and subjects with mild cognitive impairment. Neuroimage Clin 2013; 3: 39–46.

Jaggumantri S, Dunbar M, Edgar V, Mignone C, Newlove T, Elango R, et al. Treatment of Creatine Transporter (SLC6A8) Deficiency With Oral S-Adenosyl Methionine as Adjunct to L-arginine, Glycine, and Creatine Supplements. Pediatr Neurol 2015; 53: 360–363.e2.

Jensen O, Mazaheri A. Shaping functional architecture by oscillatory alpha activity: gating by inhibition. Front Hum Neurosci 2010; 4: 186.

Jensen O, Tesche CD. Frontal theta activity in humans increases with memory load in a working memory task. Eur J Neurosci 2002; 15: 1395–1399.

Jeste SS, Frohlich J, Loo SK. Electrophysiological biomarkers of diagnosis and outcome in neurodevelopmental disorders. Curr Opin Neurol 2015; 28: 110–116.

Kadam SD, D'Ambrosio R, Duveau V, Roucard C, Garcia-Cairasco N, Ikeda A, de Curtis M, et al. Methodological Standards and Interpretation of Video-Electroencephalography in Adult Control Rodents. A TASK1-WG1 Report of the AES/ILAE Translational Task Force of the ILAE. Epilepsia 2017; 58: 10-27.

van de Kamp JM, Mancini GM, Salomons GS. X-linked creatine transporter deficiency: clinical aspects and pathophysiology. J Inherit Metab Dis 2014; 37: 715–733.

Klimesch W, Sauseng P, Hanslmayr S, Gruber W, Freunberger R. Event-related phase reorganization may explain evoked neural dynamics. Neurosci Biobehav Rev 2007; 31: 1003–1016.

Kurosawa Y, Degrauw TJ, Lindquist DM, Blanco VM, Pyne-Geithman GJ, Daikoku T, et al. Cyclocreatine treatment improves cognition in mice with creatine transporter deficiency. J Clin Invest 2012; 122: 2837–2846.

LeBlanc JJ, DeGregorio G, Centofante E, Vogel-Farley VK, Barnes K, Kaufmann WE, et al. Visual evoked potentials detect cortical processing deficits in Rett syndrome. Ann Neurol 2015; 78: 775–786.

Downloaded from https://academic.oup.com/braincomms/advance-article/doi/10.1093/braincomms/fcaa089/5866973 by guest on 16 August 2020

Leuzzi V, Mastrangelo M, Battini R, Cioni G. Inborn errors of creatine metabolism and epilepsy. Epilepsia 2013; 54: 217–227.

Lloyd-Fox S, Blasi A, Elwell CE. Illuminating the developing brain: the past, present and future of functional near infrared spectroscopy. Neurosci Biobehav Rev 2010; 34: 269–284.

Lupori L, Sagona G, Fuchs C, Mazziotti R, Stefanov A, Putignano E, et al. Site-specific abnormalities in the visual system of a mouse model of CDKL5 deficiency disorder [Internet]. Hum Mol Genet 2019Available from: http://dx.doi.org/10.1093/hmg/ddz102

Maheshwari A, Marks RL, Yu KM, Noebels JL. Shift in interictal relative gamma power as a novel biomarker for drug response in two mouse models of absence epilepsy. Epilepsia 2016; 57: 79–88.

Mak CSW, Waldvogel HJ, Dodd JR, Gilbert RT, Lowe MTJ, Birch NP, et al. Immunohistochemical localisation of the creatine transporter in the rat brain. Neuroscience 2009; 163: 571–585.

Mancardi MM, Caruso U, Schiaffino MC, Baglietto MG, Rossi A, Battaglia FM, et al. Severe epilepsy in X-linked creatine transporter defect (CRTR-D). Epilepsia 2007; 48: 1211–1213.

Mazziotti R, Lupori L, Sagona G, Gennaro M, Della Sala G, Putignano E, et al. Searching for biomarkers of CDKL5 disorder: early-onset visual impairment in CDKL5 mutant mice. Hum Mol Genet 2017; 26: 2290–2298.

Mercimek-Mahmutoglu S, Connolly MB, Poskitt KJ, Horvath GA, Lowry N, Salomons GS, et al. Treatment of intractable epilepsy in a female with SLC6A8 deficiency. Mol Genet Metab 2010; 101: 409–412.

Milikovsky DZ, Weissberg I, Kamintsky L, Lippman K, Schefenbauer O, Frigerio F, et al. Theta rhythm alterations – a novel predictive biomarker of epilepsy. Journal of the Neurological Sciences 2017; 381: 86.

Downloaded from https://academic.oup.com/braincomms/advance-article/doi/10.1093/braincomms/fcaa089/5866973 by guest on 16 August 2020

Molinaro A, Alessandrì MG, Putignano E, Leuzzi V, Cioni G, Baroncelli L, et al. A Nervous System-Specific Model of Creatine Transporter Deficiency Recapitulates the Cognitive Endophenotype of the Disease: a Longitudinal Study. Sci Rep 2019; 9: 62.

Müller M, Can K. Aberrant redox homoeostasis and mitochondrial dysfunction in Rett syndrome. Biochemical Society Transactions 2014; 42: 959–964.

Nash SR, Giros B, Kingsmore SF, Rochelle JM, Suter ST, Gregor P, et al. Cloning, pharmacological characterization, and genomic localization of the human creatine transporter. Receptors Channels 1994; 2: 165–174.

Nelson CA 3rd, McCleery JP. Use of event-related potentials in the study of typical and atypical development. J Am Acad Child Adolesc Psychiatry 2008; 47: 1252–1261.

Nicolás B, Sala-Padró J, Cucurell D, Santurino M, Falip M, Fuentemilla L. Theta rhythm supports hippocampus-dependent integrative encoding in schematic memory networks. Available from: http://dx.doi.org/10.1101/2019.12.16.874024

Póo P, Arias A, Vilaseca MA, Ribes A, Artuch R, Sans A, et al. X-linked creatine transporter deficiency in two patients with severe mental retardation and autism. J Inherit Metab Dis 2006; 29:220-223.

Racine RJ. Modification of seizure activity by electrical stimulation. II. Motor seizure. Electroencephalogr Clin Neurophysiol 1972; 32: 281–294.

Rose S, Niyazov DM, Rossignol DA, Goldenthal M, Kahler SG, Frye RE. Clinical and Molecular Characteristics of Mitochondrial Dysfunction in Autism Spectrum Disorder. Mol Diagn Ther 2018; 22: 571–593.

Schiaffino MC, Bellini C, Costabello L, Caruso U, Jakobs C, Salomons GS, et al. X-linked creatine transporter deficiency: clinical description of a patient with a novel SLC6A8 gene mutation. Neurogenetics 2005; 6: 165–168.

Sinclair D, Oranje B, Razak KA, Siegel SJ, Schmid S. Sensory processing in autism spectrum disorders and Fragile X syndrome-From the clinic to animal models. Neurosci Biobehav Rev 2017;

Downloaded from https://academic.oup.com/braincomms/advance-article/doi/10.1093/braincomms/fcaa089/5866973 by guest on 16 August 2020

76: 235–253.

Skelton MR, Schaefer TL, Graham DL, Degrauw TJ, Clark JF, Williams MT, et al. Creatine transporter (CrT; Slc6a8) knockout mice as a model of human CrT deficiency. PLoS One 2011; 6: e16187.

Summerfield C, Egner T. Expectation (and attention) in visual cognition. Trends Cogn Sci 2009; 13: 403–409.

Udobi KC, Kokenge AN, Hautman ER, Ullio G, Coene J, Williams MT, et al. Cognitive deficits and increases in creatine precursors in a brain-specific knockout of the creatine transporter gene Slc6a8. Genes Brain Behav 2018; 17: e12461.

Uhlhaas PJ, Pipa G, Lima B, Melloni L, Neuenschwander S, Nikolić D, et al. Neural synchrony in cortical networks: history, concept and current status. Front Integr Neurosci 2009; 3: 17.

Valayannopoulos V, Boddaert N, Chabli A, Barbier V, Desguerre I, Philippe A, et al. Treatment by oral creatine, L-arginine and L-glycine in six severely affected patients with creatine transporter defect. J Inherit Metab Dis 2012; 35: 151–157.

Vanderwert RE, Nelson CA. The use of near-infrared spectroscopy in the study of typical and atypical development. NeuroImage 2014; 85: 264–271.

Watts ME, Pocock R, Claudianos C. Brain Energy and Oxygen Metabolism: Emerging Role in Normal Function and Disease. Front Mol Neurosci 2018; 11: 216.

Willoughby JO, Fitzgibbon SP, Pope KJ, Mackenzie L, Medvedev AV, Clark CR, et al. Persistent abnormality detected in the non-ictal electroencephalogram in primary generalised epilepsy. J Neurol Neurosurg Psychiatry 2003; 74: 51–55.

Downloaded from https://academic.oup.com/braincomms/advance-article/doi/10.1093/braincomms/fcaa089/5866973 by guest on 16 August 2020

Figure legends

Fig. 1. Altered neural oscillations in CrT$^{-/y}$ mice and CTD patients. (A) Schematic diagram of the apparatus used for video-EEG recordings in awake, freely-moving mice. EEG recordings were performed at PND200. For baseline EEG analysis, signals were segmented in 30-s epochs. The vigilance state in each epoch was manually classified as active wake, passive wake or sleep, based on the inspection of video recordings. EEG signals were converted into power spectra by Fast Fourier Transform (FFT) for at least 12 epochs in each light/dark cycle and wake/sleep condition. Consecutive epochs of the same vigilance state were selected to be spaced at least 10 minutes apart between each other. The spectra were normalized to the total power of the signal. The power spectra were averaged over subjects in each light/dark cycle and wake/sleep condition at frequency ranges divided into five bands as follows: 0.5–4 (delta), 4–8 (theta), 8–12 (alpha), 12–30 (beta), and 30–45 (gamma) Hz. **(B)** The patch color indicates the relative difference between WT (n = 22) and CrT$^{-/y}$ mice (n = 24) in the amplitude of EEG power bands, measured in three different behavioural states (active wake, passive wake and sleep) both during the day and the night phase. A single asterisk or a triple asterisk in the colored patch indicates $p < 0.05$ and $p < 0.001$ (multiple t-test, corrected using the Benjamini, Krieger and Yekutieli procedure), respectively. **(C)** Schematic diagram of electrode location in the 10-20 international system for EEG recordings. We used this electrode configuration for EEG recordings in CTD patients and age-matched controls. The mean age of CTD patients was 7.2 years (SD = 1.8 years); for controls the mean age was 7.7 years (SD = 2.3 years). Electrodes used for the analysis were FP1 (frontopolar 1), C3 (central 3), T3 (temporal 3) and O1 (occipital 1). EEG recordings were screened and divided into artefact-free segments (10-s duration for eyes closed condition, 20-s duration for eyes open and sleep conditions). EEG signal was then exported in European Data Format (EDF) and subjected to FFT. Power spectra were estimated by averaging at least 8 segments for each behavioral state. The spectral power values in the same frequency bands described above for mice were evaluated in humans. The spectra were normalized to the total power of the signal. **(D)** The patch color indicates the relative difference between healthy controls (n = 12) and CTD patients (n = 5) in the amplitude of EEG power bands, measured in three different behavioural states (eyes open, eyes closed and sleep). A single asterisk or a double asterisk in the colored patch indicates $p < 0.05$ and $p < 0.01$ (multiple t-test), respectively. Representative EEG traces and power spectrum plots are also shown.

Fig. 2. Spontaneous epileptic phenotype in CrT$^{-/y}$ animals and stratification of EEG power data according to this phenotype. (A) Using baseline EEG recordings (24h), we found that 30% of CrT$^{-/y}$ mice (n = 24) display spontaneous seizures, while no ictal events were detected in WT

Downloaded from https://academic.oup.com/braincomms/advance-article/doi/10.1093/braincomms/fcaa089/5866973 by guest on 16 August 2020

animals (n = 22). On the right, a representative seizure in a $CrT^{-/y}$ mouse is shown. Calibration bar: 100 μV, 10s. **(B)** Frequency of spontaneous seizures in $CrT^{-/y}$ epileptic animals. **(C)** Average duration of spontaneous seizures in $CrT^{-/y}$ epileptic animals. **(D-I)** Violin plots with individual values (filled circles) depict normalized theta power spectrum of cortical EEG recordings from epileptic ($CrT^{-/y\ seiz}$, n = 7) and non-epileptic $CrT^{-/y}$ mice ($CrT^{-/y}$, n = 17). Decreased power of 4-8 Hz theta frequency band in epileptic $CrT^{-/y}$ mice during the passive wakefulness and sleep in the light phase, and during the active and passive wakefulness in the dark phase. Multiple t-tests with adjusted p-value: * $p < 0.05$, ** $p < 0.01$. Error bars, SD.

Fig. 3. Kainic acid (KA) challenge in the brain of $CrT^{-/y}$ mice. (A) Kainic acid injection (10 mg/kg) induced overt seizures in 100% of $CrT^{-/y}$ mice (n = 24), whereas only 14/22 WT animals displayed epileptic bursts at electrographical level over 1h of observation. **(B)** Effect of KA treatment at the behavioural level. Circles represent the maximum seizure rating score of individual WT and $CrT^{-/y}$ mice over a period of 1 hr after KA administration. Black lines represent mean with 95% CI. $CrT^{-/y}$ mice displayed a higher Racine score (t-test, $p < 0.001$). **(C-F)** Severity of KA-induced seizures in WT and $CrT^{-/y}$ mice at electrophysiological level. EEG analysis was performed on the same animals used for behavioural scoring. $CrT^{-/y}$ mice showed a lower latency to the first seizure (C, t-test, $p < 0.001$), and increased frequency (D, t-test, $p < 0.001$) and duration E, t-test, $p < 0.05$) of seizure events with respect to age-matched littermates. For WT animals not presenting seizures during the 1h of monitoring, we extended the observation until the occurrence of the first electrographical burst to provide a latency value. Circles represent single data values; black lines indicate mean with 95% CI. Relative percentage of tonic, clonic and tonic-clonic seizures WT and $CrT^{-/y}$ mice (F) indicates that seizure severity is more pronounced in $CrT^{-/y}$ animals (χ^2 test; $p < 0.001$). * $p < 0.05$, *** $p < 0.001$.

Fig. 4. Altered hemodynamic response in $CrT^{-/y}$ animals. (A) Typical IOS response to visual stimulation in the binocular visual field for a WT ($CrT^{+/y}$) and a $CrT^{-/y}$ animal. The Look Up Table is shown on the right. Scale bar: 1.8mm. **(B)** Contrast-response function for contralateral eye stimulation in male WT (n = 6) and $CrT^{-/y}$ (n = 9) mice at PND40. IOS amplitude was increased in $CrT^{-/y}$ animals in particular at high contrast of visual stimuli (Two-way ANOVA, effect of genotype $p < 0.05$, genotype x contrast interaction $p < 0.05$, post- hoc Holm Sidak method, $p < 0.01$ at 90% of contrast). **(C)** Response for contralateral eye stimulation in male WT and $CrT^{-/y}$ mice at three different time points (PND40, PND110 and PND180; n = 15 for each group at PND40 and PND110, n = 19 at PND180). IOS amplitude was significantly increased in $CrT^{-/y}$ animals (Two-

Downloaded from https://academic.oup.com/braincomms/advance-article/doi/10.1093/braincomms/fcaa089/5866973 by guest on 16 August 2020

way ANOVA, effect of genotype $p < 0.001$, post-hoc Holm Sidak method $p < 0.001$ at all ages tested). **(D)** The latency of IOS responses was longer in $CrT^{-/y}$ mice at PND110 and PND180 (Two-way ANOVA, effect of genotype $p < 0.001$, post-hoc Holm Sidak method $p < 0.001$). **(E-F)** No differences in VEP amplitude (E) and latency (F) were detected between WT (n = 10) and $CrT^{-/y}$ animals (n = 7; t-test, $p = 0.767$ and $p = 0.087$, respectively) at PND110. For all panels, circles represent single data values; black lines indicate mean with 95% CI. Representative VEP traces for a WT (continuous black line) and a $CrT^{-/y}$ (dashed blue line) mouse are also shown on the right. ** $p < 0.01$, *** $p < 0.001$. Error bars, SEM.

Fig. 5. Random Forest analysis of the dataset. (A) Scatter plot of all the experimental subjects analyzed with the full dataset (Full), behavioural (Behaviour), IOS imaging (IOS) and EEG variables plotted in the space of the first two principal components of PCA. **(B)** Comparison of accuracy for different Random Forest classifiers trained and tested, respectively, with the entire dataset, behavioural, IOS, EEG variables and randomly permuted dataset (Bootstrap). A Kruskal-Wallis analysis followed by Dunn's multiple comparisons revealed that the behavioural variable has an accuracy comparable to the full dataset, whereas the accuracy of IOS and EEG variables is slightly lower. All classifiers displayed a higher accuracy than Bootstrap ($p < 0.001$ for all comparisons). Error bars, SD. **(C)** Histogram depicts the relative importance of top 14 features in the Random Forest model. The following abbreviations were used: ios-amp, amplitude of IOS signal; naw, night active wake; rot, rotarod; dpw, day passive wake; ds, day sleep; ios-lat, latency of IOS signal; mwm-train, training distance of Morris water maze; ns, night sleep; npw, night passive wake; daw, day active wake; KAfreq, frequency of seizures after KA challenge. * $p < 0.05$, ** $p < 0.01$, *** $p < 0.001$, ns, not significant.

Video 1. Representative video recording of a clonic seizure (Racine stage 3) in a $CrT^{-/y}$ animal.

Video 2. Representative video recording of a tonic-clonic seizure (Racine stage 6) in a $CrT^{-/y}$ animal.

Downloaded from https://academic.oup.com/braincomms/advance-article/doi/10.1093/braincomms/fcaa089/5866973 by guest on 16 August 2020

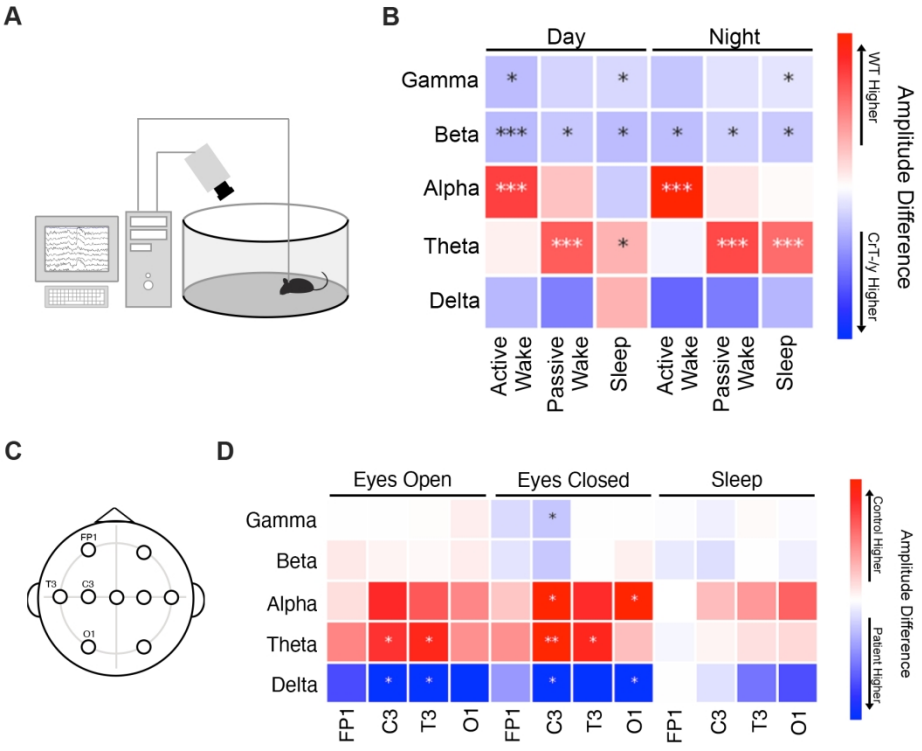

Figure 1

Downloaded from https://academic.oup.com/braincomms/advance-article/doi/10.1093/braincomms/fcaa089/5866973 by guest on 16 August 2020

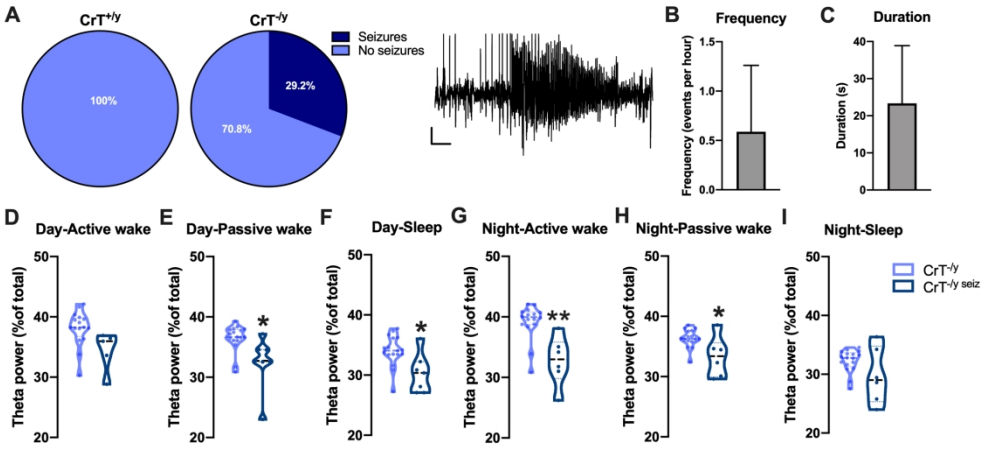

Figure 2

196x89mm (300 x 300 DPI)

Downloaded from https://academic.oup.com/braincomms/advance-article/doi/10.1093/braincomms/fcaa089/5866973 by guest on 16 August 2020

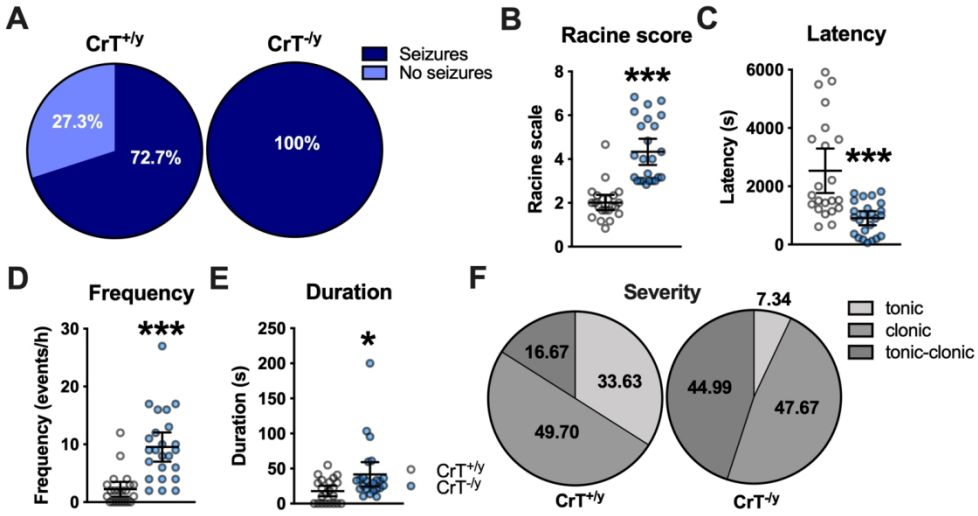

Figure 3

135x73mm (300 x 300 DPI)

Downloaded from https://academic.oup.com/braincomms/advance-article/doi/10.1093/braincomms/fcaa089/5866973 by guest on 16 August 2020

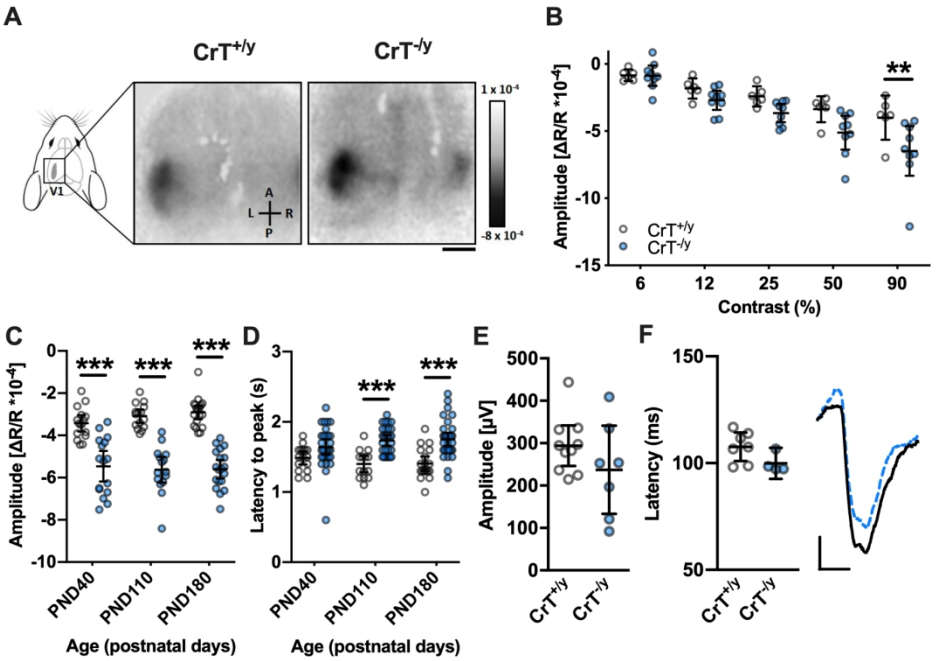

Figure 4

166x113mm (300 x 300 DPI)

Downloaded from https://academic.oup.com/braincomms/advance-article/doi/10.1093/braincomms/fcaa089/5866973 by guest on 16 August 2020

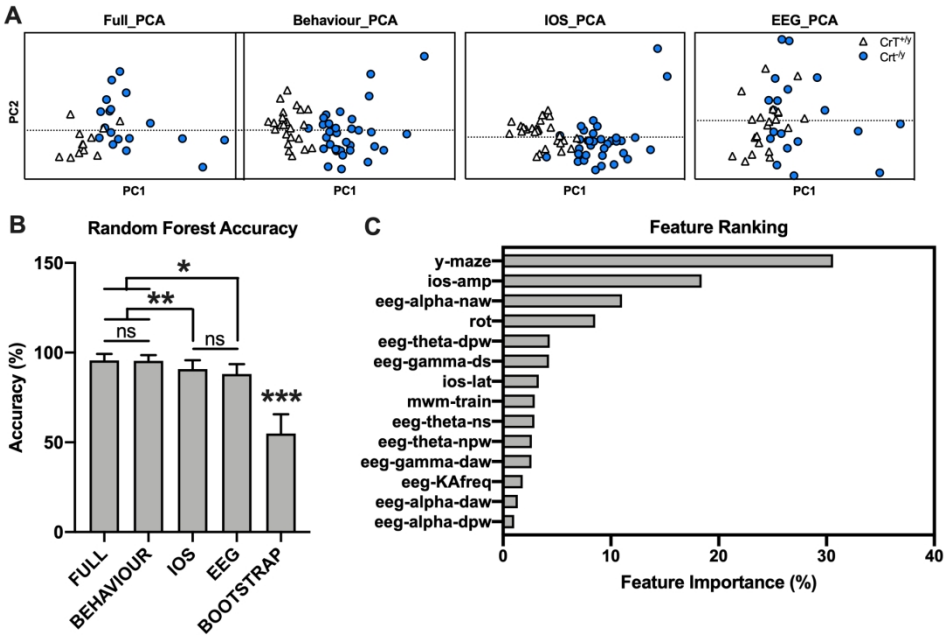

Figure 5

173x115mm (300 x 300 DPI)

Downloaded from https://academic.oup.com/braincomms/advance-article/doi/10.1093/braincomms/fcaa089/5866973 by guest on 16 August 2020

Table 1. Clinical and demographic characteristics of patients with CTD

Patient n° /gender	Age (years)/ seizure type at onset	Age (years) at EEG	Age (years) at last follow-up	Biochemical value (Cr/Crn; n.v. < 1.0)	Genetic testing (*Slc6a8* mutation)
1/M	5.0/ focal motor	8.4	22.7	2.35	c. 1006-1008 del AAC(de novo)
2/M	0.4/spasms	8.3	15.8	3.6	IV s1-2A >G
3/M	No seizures	5.5	15.6	3.08	c.757 G>C (inherited)
4/M	No seizures	9.0	8.3	2.12	p.Val246Cysfs*47
5/M	1.3/focal to bilateral	5.1	7.5	3.5	c.1376T>C, p.Leu459Pro

Abbreviations: CTD- Creatine Transporter Deficiency; Cr- Creatine: Crn: Creatinine; M: male.

Downloaded from https://academic.oup.com/braincomms/advance-article/doi/10.1093/braincomms/fcaa089/5866973 by guest on 16 August 2020

Creatine transporter deficiency is an orphan disorder characterized by intellectual disability, autistic-like behavior and epilepsy. Mazziotti et al. identified quantitative biomarkers of translational value for monitoring disease progression and response to therapeutics.

Downloaded from https://academic.oup.com/braincomms/advance-article/doi/10.1093/braincomms/fcaa089/5866973 by guest on 16 August 2020

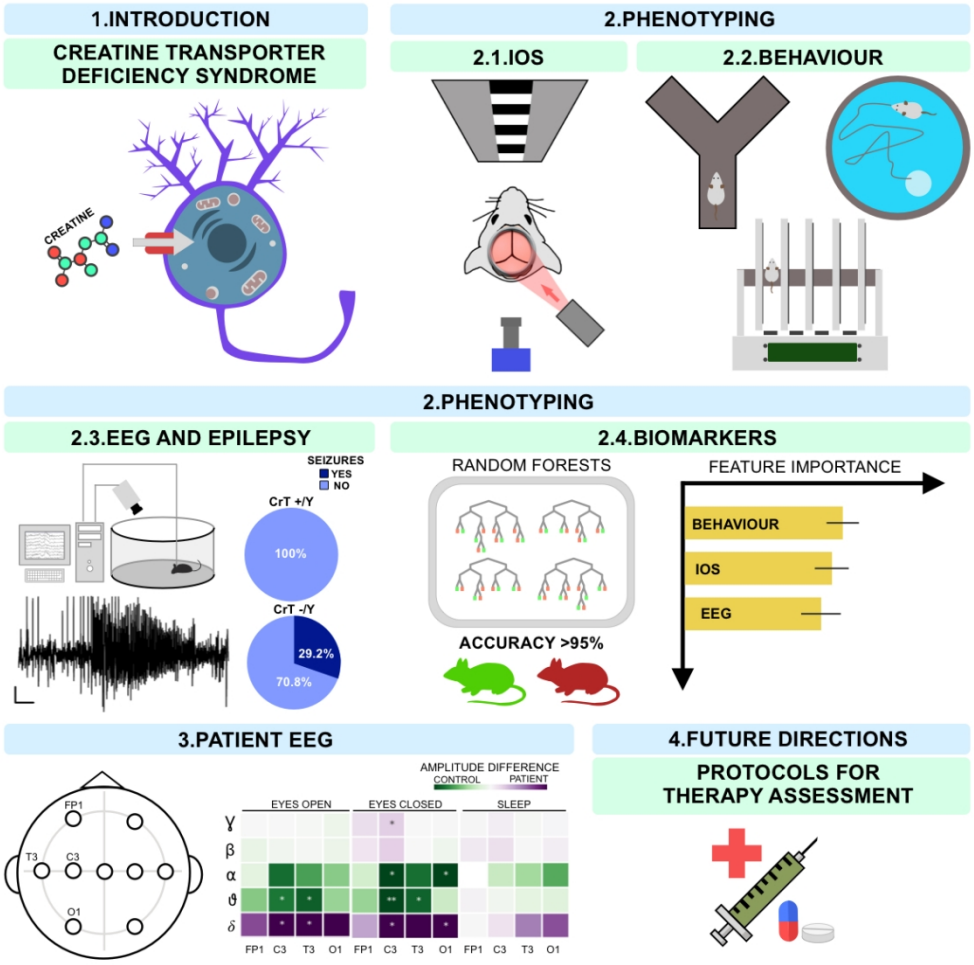

Graphical abstract

423x423mm (72 x 72 DPI)

Downloaded from https://academic.oup.com/braincomms/advance-article/doi/10.1093/braincomms/fcaa089/5866973 by guest on 16 August 2020